The AIRCRAFT ENGINEER

"FLIGHT" ENGINEERING SECTION

Edited by C. M. POULSEN

No. 114 (Volume XI No. 1) 10th Year July 25, 1935

# FAIRING LINES

*With the Increasing Use of Streamline Bodies the Question of Accurate "Lines" Assumes Considerable Importance : This Article Outlines a Mathematical Method Which Can be Used as an Alternative to the Shipbuilder's Setting Out of the Lines Full-size in the Loft*

By A. E. RUSSELL, B.Sc.

THE "shape" of streamline bodies is becoming more and more important. Not only do "hollows" or "flats" tend towards a loss of aerodynamic efficiency but they offend against the critic's eye to an extent that may be even more important than their aerodynamic effect. It has sometimes been possible to correct these blemishes by simply altering fairing formers and stringers, but with some modern forms of monocoque construction these alterations are not so easy; it becomes even more important that the fairing lines evolved in the drawing office should be correct the first time.

In the past the usual method has been to set out on the drawing board cross-sections along the length of the body and run surface lines in elevation and plan. The fact that these lines are smooth in elevation does not necessarily mean that the "water lines" are smooth. Indeed, when both these are correct radial lines should also be checked. The process has been one of trial and error involving a considerable amount of time.

In the method outlined here, absolute confidence may be placed in the results and the time taken is reduced to a small percentage of that required by the usual methods.

The principle is as follows.

In Fig. 1 an arbitrary curve has been drawn—Curve A. This curve may be represented by an equation of the form

$$y = f(x)$$

A family of curves may be related to this in the form

$$y^n = f(x)$$

The calculation is as follows :—

At selected values of $x$ read the corresponding values of the ordinates. Find the logarithm of the ordinate and multiply by a trial value of "$n$." In Table 1 the values

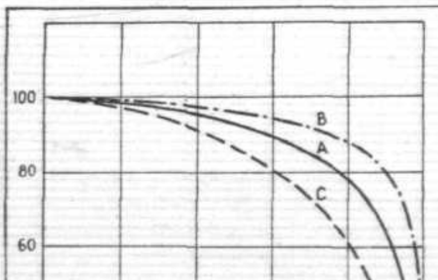


FIG. 1.

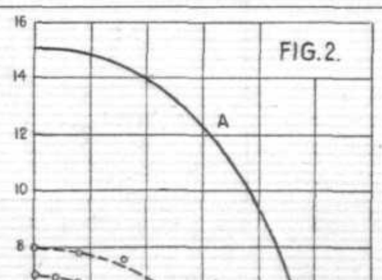


FIG. 2.

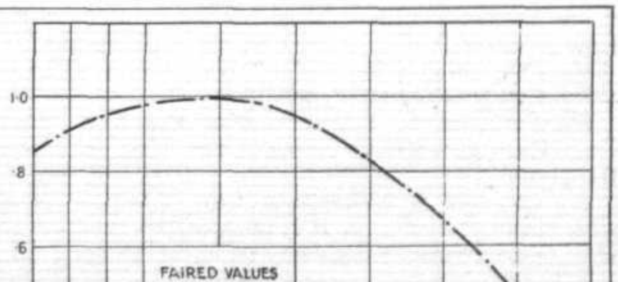


FIG. 3.

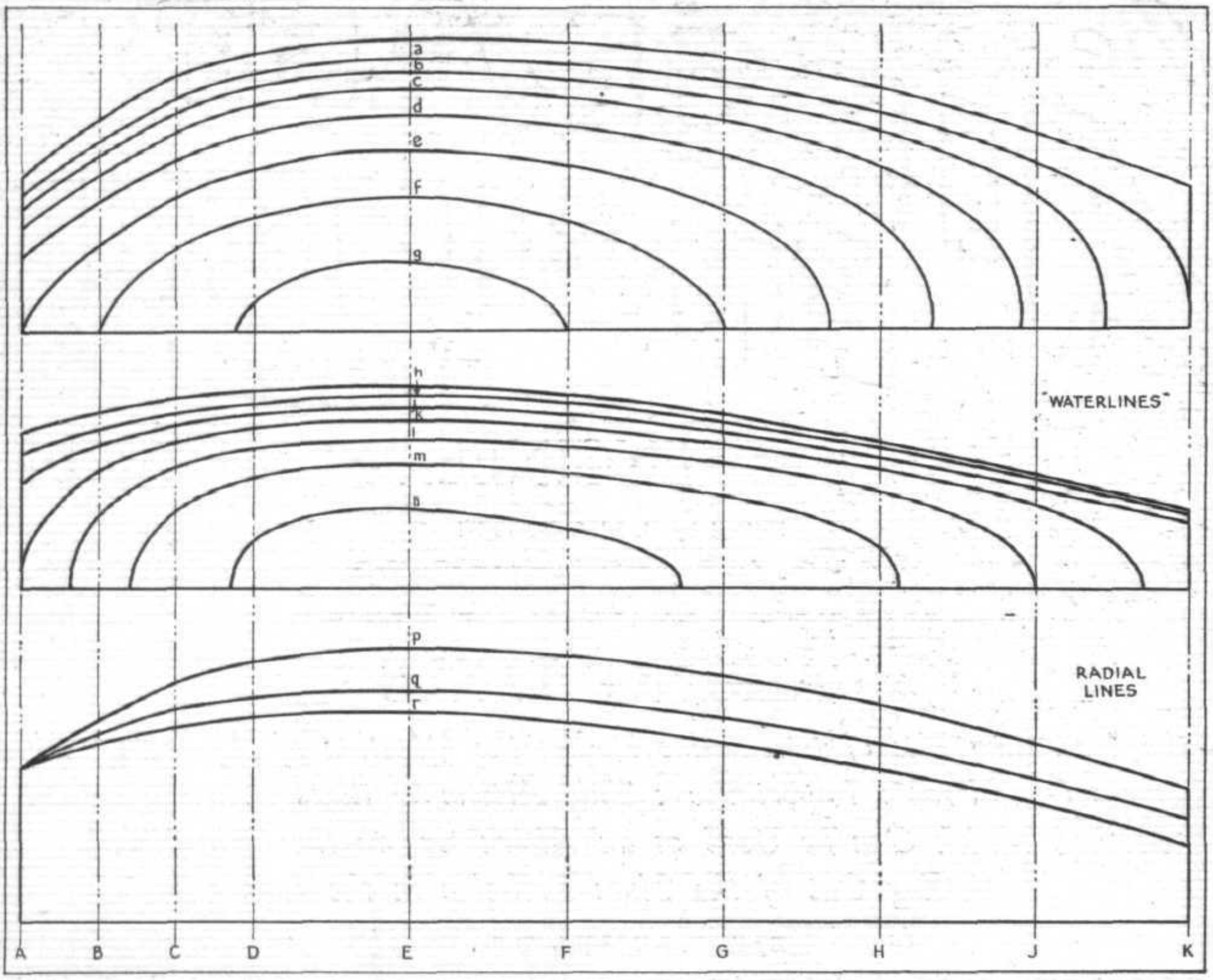


of "$n$" used are 0.5 and 2.0. The values of the antilogarithms give the new curve.

TABLE 1.

| (1) $x$ | (2) $y$ Curve A. | (3) log $y$. | (4) 0.5 log 5 ($n$ = 0.5). | (5) Antilog (4) Curve B. | (6) 2 log $y$ ($n$ = 2). | (7) Antilog (6) Curve C. |
|---|---|---|---|---|---|---|
| 0 | 100.0 | 2.0 | 1.0 | 10.0 | 4.0 | 10,000 |
| 0.2 | 98.8 | 1.9948 | 0.9974 | 9.94 | 3.9896 | 9,770 |
| 0.4 | 95.5 | 1.9800 | 0.9900 | 9.77 | 3.9600 | 9,120 |
| 0.6 | 89.8 | 1.9533 | 0.9766 | 9.48 | 3.9066 | 8,070 |
| 0.7 | 85.0 | 1.9294 | 0.9647 | 9.22 | 3.8588 | 7,230 |
| 0.8 | 78.2 | 1.8932 | 0.9466 | 8.85 | 3.7864 | 6,110 |
| 0.9 | 64.5 | 1.8096 | 0.9048 | 8.03 | 3.6192 | 4,160 |
| 0.95 | 51.0 | 1.7076 | 0.8538 | 7.14 | 3.4152 | 2,600 |
| 0.975 | 40.0 | 1.6020 | 0.8010 | 6.32 | 3.2040 | 1,600 |
| 1.0 | 0 | 0 | 0 | 0 | 0 | 0 |

The curves B and C have been corrected to the same scale as curve A and plotted on the same graph.

By a suitable choice of "$n$" the curve may be made to cover a wide range of shapes.

Furthermore, by fore-shortening the $x$ or $y$ axes, very dissimilar geometric forms may be mathematically translated.

An example will illustrate this clearly. Commencing with curve A of Fig. 2, it is required to produce a section very approximately the same as curve B.

The calculation is shown below.

TABLE 2.

| | | | | | | | | | | |
|---|---|---|---|---|---|---|---|---|---|---|
| $x$ | 0 | 0.2 | 0.4 | 0.6 | 0.7 | 0.8 | 0.9 | 0.95 | 0.975 | 1.0 |
| | 0 | 2.12 | 4.24 | 6.36 | 7.42 | 8.48 | 9.54 | 10.07 | 10.33 | 10.6 |
| y | 15.0 | 14.70 | 13.90 | 11.97 | 10.35 | 8.35 | 5.30 | 3.30 | 2.00 | 0 |
| log y | 1.1761 | 1.1673 | 1.1430 | 1.0781 | 1.0150 | 0.9217 | 0.7243 | 0.5185 | 0.3010 | 0 |
| $n$ log y | 0.2931 | 0.2909 | 0.2848 | 0.2687 | 0.2529 | 0.2297 | 0.1805 | 0.1292 | 0.0750 | 0 |
| Antilog | 1.964 | 1.949 | 1.927 | 1.857 | 1.790 | 1.697 | 1.515 | 1.346 | 0.5623 | 0 |
| $y$ | 7.0 | 6.95 | 6.87 | 6.62 | 6.38 | 6.05 | 5.40 | 4.80 | 2.00 | 0 |

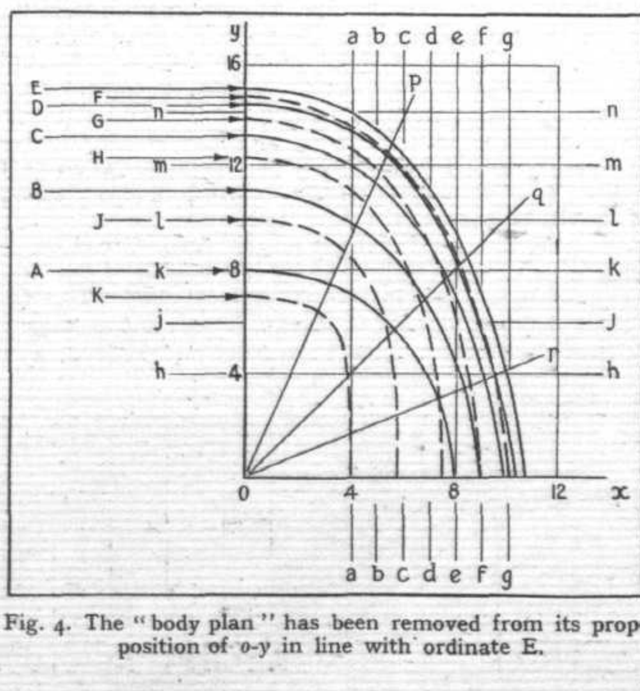


**Fig. 4. The "body plan" has been removed from its proper position of o-y in line with ordinate E.**

Select some value of $x$ of curve B

say, $x = 0.8 = 3.2''$ $y = 6.05''$

For equal maximum ordinates the equivalent position on curve A would be $\frac{15 \times 6.05}{7.0} = 12.96$.

Let $n$ be the index necessary to translate the shape.

The new ordinate at $x = 0$ is Antilog $n \times 1.1761$.

" " " $x = 0.8$ is Antilog $n \times 0.9217$.

After reducing this new maximum ordinate to the original value the ordinate at 0.8 is

$$n \times 0.9217 \times \frac{15}{n \times 1.1761} = 12.96''$$

$$\begin{aligned} \text{or} \quad \log 15 + 0.9217n - 1.1761n &= \log 12.96 \\ 1.1761 - 0.2544n &= 1.1126 \\ \therefore \quad n &= 0.249 \end{aligned}$$

It is assumed that the new calculated spots shown on curve B are close enough to the desired shape so that the curve passing through these spots would be used.

A further calculation will be done to show how near the curve may be translated into a circle.

TABLE 3.

| | | | | | | | | | | |
|---|---|---|---|---|---|---|---|---|---|---|
| $x$ | 0 | 0.2 | 0.4 | 0.6 | 0.7 | 0.8 | 0.9 | 0.95 | 0.975 | 1.0 |
| | 0 | 2.12 | 4.24 | 6.36 | 7.42 | 8.48 | 9.54 | 10.07 | 10.33 | 10.60 |
| $y$ | 15.0 | 14.70 | 13.90 | 11.97 | 10.35 | 8.35 | 5.30 | 3.30 | 2.00 | 0 |
| log $y$ | 1.1761 | 1.1673 | 1.1430 | 1.0781 | 1.015 | 0.9217 | 0.7243 | 0.5185 | 0.3010 | 0 |
| 0.853log $y$ | 1.004 | 0.996 | 0.975 | 0.920 | 0.866 | 0.787 | 0.618 | 0.443 | 0.257 | 0 |
| Antilog | 10.1 | 9.91 | 9.44 | 8.32 | 7.34 | 6.12 | 4.15 | 2.77 | 1.81 | 0 |
| $y$ | 8.0 | 7.85 | 7.48 | 6.59 | 5.82 | 4.85 | 3.29 | 2.20 | 1.44 | 0 |

At $x = 0.8$.

$$\text{Equivalent ordinate on curve A} \doteq \frac{4.85}{8.0} \times 15 = 9.10$$

$$\begin{aligned} \therefore \quad \log 15 - 0.2544n &= \log 9.1 \\ \therefore \quad n &= 0.853 \end{aligned}$$

The limitations of the method are now apparent since it is probably not possible to get two exact chosen sections. If only one section need be exact then it is possible to approximate closely to any other.

The method will now be extended to an aerodynamic form resembling a fuselage shown in Fig. 4.

The section at A is the same as that of curve C of Fig. 2.

The section at E is the same as that of curve A of Fig. 2.

The section at K is the same as that of curve B of Fig. 2.

Only the upper part of the body is shown as a similar calculation will hold for the lower.

The shape in elevation and plan may be drawn in any arbitrary manner to suit a particular design so that the application of the method is not limited by the presence of any sudden change of slopes as is sometimes found in side elevation in the neighbourhood of the cockpit.

The calculation is shown in Table 4.

The values of "$n$" as previously found (Section A $n = 0.853$; Section BE $n = 1.000$; Section K $n = 0.249$) are faired-in on Fig. 3. Any reasonable smooth line may be selected.

The values of "$n$" at intermediate points may now be read from this graph and used in conjunction with the corresponding maximum ordinate and abscissa taken from the side elevation and plan.

Briefly, the work necessary to "fair" a fuselage is as follows:—

(*a*) Select a cross-section whose shape is fixed by internal body arrangements.

(*b*) Draw the approximate required shape at the forward end and find by trial the values of "$n$" necessary to translate the cross-section at (*a*).

(*c*) Treat the rear end similarly.

(*d*) Fair in the values of "$n$" so found for sections (*a*), (*b*) and (*c*).

(*e*) Draw the side elevation and plan to suit the aircraft layout.

(*f*) Proceed for selected cross-sections as in Table 4.

It is obvious that no great mathematical skill or ability is required and that the time required may be reckoned in hours instead of days. Furthermore, the co-ordinates of any point on the contour may be found in relation to any other.

TABLE 4.

| | | SECTION B. | | | | SECTION C. | | | | SECTION D. | | | |
|---|---|---|---|---|---|---|---|---|---|---|---|---|---|
| $x$ / $y$ / $n$ | | $x$ max. = 9.0, $y$ max. = 10.9, $n$ = 0.91 | | | | $x$ max. = 9.8, $y$ max. = 13.1, $n$ = 0.95 | | | | $x$ max. = 10.2, $y$ max. = 14.3, $n$ = 0.978 | | | |
| $x$ | log $y$. | $x$ | $n$ log $y$. | Antilog. | $y$ | $x$ | $n$ log $y$. | Antilog. | $y$ | $x$ | $n$ log $y$. | Antilog. | $y$ |
| 0 | 1.1761 | 0 | 1.0702 | 11.75 | 10.9 | 0 | 1.1174 | 13.10 | 13.10 | 0 | 1.150 | 14.12 | 14.3 |
| 0.2 | 1.1673 | 1.8 | 1.0622 | 11.54 | 10.7 | 1.96 | 1.109 | 12.85 | 12.86 | 2.04 | 1.142 | 13.87 | 14.1 |
| 0.4 | 1.1430 | 3.6 | 1.040 | 10.96 | 10.16 | 3.92 | 1.086 | 12.19 | 12.20 | 4.08 | 1.118 | 13.12 | 13.3 |
| 0.6 | 1.0781 | 5.4 | 0.9810 | 9.57 | 8.88 | 5.88 | 1.024 | 10.57 | 10.58 | 3.12 | 1.054 | 11.34 | 11.5 |
| 0.7 | 1.015 | 6.3 | 0.9236 | 8.39 | 7.78 | 6.86 | 0.964 | 9.20 | 9.20 | 7.14 | 0.993 | 9.84 | 9.96 |
| 0.8 | 0.9217 | 7.2 | 0.8388 | 6.90 | 6.40 | 7.84 | 0.876 | 7.52 | 7.52 | 8.16 | 0.901 | 7.96 | 8.06 |
| 0.9 | 0.7243 | 8.1 | 0.6592 | 4.56 | 4.24 | 8.82 | 0.688 | 4.87 | 4.88 | 9.18 | 0.708 | 5.10 | 5.17 |
| 0.95 | 0.5185 | 8.54 | 0.4718 | 2.96 | 2.74 | 9.30 | 0.493 | 3.11 | 3.10 | 9.68 | 0.507 | 3.21 | 3.25 |
| 0.975 | 0.3010 | 8.78 | 0.2740 | 1.88 | 1.74 | 9.56 | 0.286 | 1.93 | 1.93 | 9.94 | 0.294 | 1.97 | 2.00 |
| 1.0 | 0 | 9.0 | 0 | 0 | 0 | 9.80 | 0 | 0 | 0 | 10.20 | 0 | 0 | 0 |

| | SECTION F. | | | | SECTION G. | | | | SECTION H. | | | | SECTION J. | | | |
|---|---|---|---|---|---|---|---|---|---|---|---|---|---|---|---|---|
| $x$ / $y$ / $n$ | $x$ max. = 9.9, $y$ max. = 14.6, $n$ = 0.95 | | | | $x$ max. = 8.96, $y$ max. = 13.8, $n$ = 0.84 | | | | $x$ max. = 7.56, $y$ max. = 12.20, $n$ = 0.68 | | | | $x$ max. = 5.85, $y$ max. = 9.90, $n$ = 0.48 | | | |
| $x$ | $x$ | $n$ log $y$. | Antilog. | $y$ | $x$ | $n$ log $y$. | Antilog. | $y$ | $x$ | $n$ log $y$. | Antilog. | $y$ | $x$ | $n$ log $y$. | Antilog. | $y$ |
| 0 | 0 | 1.1174 | 13.10 | 14.6 | 0 | .989 | 9.75 | 13.8 | 0 | .800 | 6.31 | 12.20 | 0 | .565 | 3.67 | 9.90 |
| 0.2 | 1.98 | 1.109 | 12.85 | 14.34 | 1.8 | .982 | 9.59 | 13.58 | 1.51 | .794 | 6.22 | 12.0 | 1.17 | .560 | 3.63 | 9.79 |
| 0.4 | 3.96 | 1.086 | 12.19 | 13.60 | 3.58 | .961 | 9.14 | 12.94 | 3.02 | .777 | 5.98 | 11.6 | 2.34 | .549 | 3.54 | 9.55 |
| 0.6 | 5.94 | 1.024 | 10.57 | 11.8 | 5.38 | .907 | 8.07 | 11.42 | 4.54 | .733 | 5.41 | 10.5 | 3.51 | .517 | 3.29 | 8.88 |
| 0.7 | 6.93 | 0.964 | 9.20 | 10.26 | 6.28 | .854 | 7.14 | 10.10 | 5.30 | .690 | 4.90 | 9.47 | 4.10 | .487 | 3.07 | 8.28 |
| 0.8 | 7.74 | 0.876 | 7.52 | 8.40 | 7.16 | .775 | 5.96 | 8.44 | 6.04 | .627 | 4.23 | 8.18 | 4.68 | .443 | 2.77 | 7.47 |
| 0.9 | 8.91 | 0.688 | 4.87 | 5.44 | 8.06 | .609 | 8.12 | 5.74 | 6.80 | .493 | 3.11 | 6.01 | 5.26 | .348 | 2.23 | 6.02 |
| 0.95 | 9.41 | 0.493 | 3.11 | 3.48 | 8.52 | .436 | 2.76 | 3.86 | 7.18 | .353 | 2.25 | 4.35 | 5.56 | .249 | 1.77 | 4.78 |
| 0.975 | 9.65 | 0.286 | 1.93 | 2.16 | 8.74 | .253 | 1.79 | 2.54 | 7.38 | 205 | 1.60 | 3.09 | 5.70 | .144 | 1.39 | 3.75 |
| 1.0 | 9.90 | 0 | 0 | 0 | 8.96 | 0 | 0 | 0 | 7.56 | 0 | 0 | 0 | 5.85 | 0 | 0 | 0 |

# FOR ENGINE RESEARCH

IN the Anglo-American Oil Company's engine test laboratories last week, *Flight* inspected a most interesting new apparatus for indicating phenomena in connection with I.C. engines. It is the work of Mr. E. M. Dodds, in conjunction with Metropolitan-Vickers, Ltd.

The Metrovick-Dodds indicator seeks to overcome the disadvantages of mechanical methods of engine performance indication—inertia, lost motion, etc. Very briefly, it consists essentially of a thin stainless steel diaphragm arranged in the head of the engine under test. The diaphragm transmits the pressure fluctuations to a water-cooled carbon pile resistance, which is utilised to energise the deflecting coils of a cathode-ray tube.

Thus, pressure variations in the cylinder become current variations which deflect the cathode ray spot vertically on the fluorescent screen of the tube.

In addition, a contact breaker is arranged to move the beam spot horizontally at a rate proportional to the crank angle. The combination of the relatively perpendicular pressure and time motions causes the spot to trace out the PT diagram.

Uses of the indicator include the following:—

The taking of PV and PT diagrams for petrol and diesel engines; the securing of ionisation oscillograms—leading to the determination of time of passage and duration of the flame front; the study of detonation problems; and the determination of the pressure in the oil fuel line of a diesel engine, and also of following the motion of the injection needle valve—even this is accomplished without mechanical contact.

Individual cycles are demonstrated, so that it is easy to test the steadiness of running of an engine. Any small portion of the cycle can be magnified, while diagrams may be taken at any required engine speed, and can be observed visually, traced or photographed.

The apparatus, which is compact and easily portable, is to be marketed by Metropolitan-Vickers, Ltd., of Manchester, at a price in the region of £80.

# A NEW METHOD of STRESSING WOODEN SPARS

## *A Method of Determining the Moment of Rupture of Wooden Members which Takes Into Account the Different Properties of Wood in Tension and Compression*

By PROFESSOR W. PRAGER, of Istanbul University

At the Fourth International Congress for Applied Mechanics, held in July of last year, at Cambridge, Prof. W. Prager gave an account of a method of "stressing" wooden spars, of exceptional interest to designers. The attractions of the method lie in its accuracy, as it takes into account the "form factor" of the spar, and in its simplicity, since it enables the dimensions of a spar to be determined directly for any required bending moment without necessitating a number of trial or preliminary computations. A description of the method has since been published in German (W. Prager: "Ein neues Verfahren zur Bemessung auf Biegung beanspruchter Holzstäbe"—*Schweizer Bauzeitung*, November 3rd, 1934) but no account has yet been available in English. [The Editor is indebted to Mr. N. A. de Bruyne, M.A., Ph.D., of Aero Research Ltd., Duxford, for calling his attention to the Prager method.]

### *The Prager Method*

In computing the dimensions of beams it is customary to use formulæ which are based on a linear distribution of the stresses over the cross-section of the beam. The dimensions of the beam are so selected that the maximum stress given by such formulæ just reaches a stress which is regarded as permissible. The ratio of the strength of the material to this admissible stress is frequently termed "safety." In a material which does not obey Hooke's law up to fracture, however, this ratio is different from the only ratio which can be described as "safe" between the bending moment at fracture and the maximum bending moment occurring during working. For determining the "safety" it is therefore necessary to ascertain the bending moment at fracture for the form of cross-section selected. We shall now describe a process for calculating the bending moment at fracture of a wooden member, with given values of tensile strength $K_z$ and compressive strength $K_D$ of the wood.

Fig. 1 shows a typical extension-compression (stress-strain) diagram for wood. When subjected to tensile stress the relation between tension and extension is linear almost up to fracture. When under compressive stress, however, a linear connection between stress and compression is present only up to a certain stress. Beyond this point a small increase in the compressive stress produces a large increase in the strain.

Fig. 2 shows an idealised stress-strain diagram, and this we shall take as the basis for our discussion. We shall examine the behaviour of a member subjected to bending stress and consisting of a material with the characteristics of the stress-strain diagram (Fig. 2), assuming that plane cross-sections are not distorted. While the bending moment gradually increases, this linear distribution of stress over the cross-section corresponds at first to a linear distribution, until in the fibres which are subjected to the highest pressure the limit of stress $K_D$ is reached. When the bending moment is further increased, we get the distribution of stress shown in Fig. 3*a*. On further increasing the bending moment the turning point E of the distribution of stress is displaced towards the tension side and the maximum tensile stress is increased.

Finally fracture occurs, either when the tensile strength $K_z$ of the material is reached on the tension side (Fig. 3*b*) or when the compression on the pressure side reaches a certain dangerous figure. For, as with the increase in the bending moment the zero line of the distribution of stresses is displaced towards the tension side, the maximum compression increases more rapidly than the maximum extension and may reach a dangerous figure even before the maximum tensile stress attains the tensile strength of the material.

We shall now deal with the first type of fracture, at which the tensile strength of the material is just reached on the tension side. We assume that the cross-section of the member has a symmetrical axis and that the plane of the bending moment coincides with the plane determined by the symmetrical axis and the axis of the member. The zero line of the distribution of stresses is then vertical to the symmetrical axis. As both the edge stresses acquire, at the moment of fracture, the known values $K_z$ and $K_D$, the distribution of stresses can already be clearly determined by indicating the position of the turning point E. The distance of this point from the extreme tension-fibre *b-b* is indicated by $x_0$ (Fig. 4). The distribution of stresses in Fig. 4 can be made up of the triangular stress distribution EFD and the rectangular stress distribution

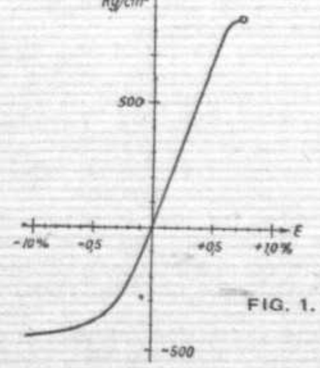


FIG. 1.

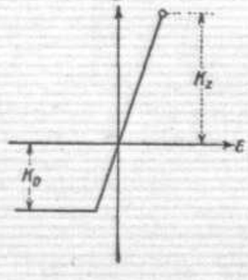


FIG. 2.

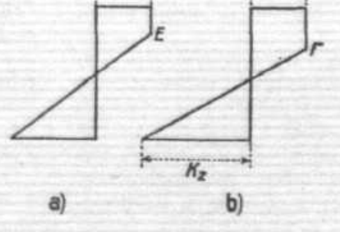


FIG. 3.

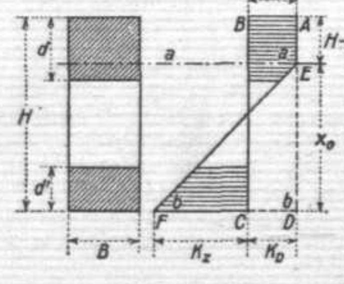


FIG. 4.

ABCD. The stress in the space $x$ from the fibre $b$-$b$ is therefore given by:

$$\sigma(x) = (K_z + K_D)\frac{x_0 - x}{x_0} - K_D \quad .. \quad .. \quad (1)$$

These stresses must be in equilibrium with the bending moment M. Accordingly:

$$\int \sigma(x)\, d\,F = 0 \text{ and } \int x\sigma(x)\, d\,F = M \quad .. \quad (2)$$

wherein $dF$ denotes the surface element of the cross-section of the member and the integration extends over the entire cross-section. If F indicates the surface of the cross-section of the member and $F_0$ the surface of the cross-section part represented by $0 \leq x \leq x_0$, and if, furthermore, in relation to the axis $b$-$b$, $\overline{S}$ is the static moment of the cross-section, $S_0$ the static moment of the cross-section part $0 \leq x \leq x_0$ and $J_0$ the moment of inertia of the cross-section part $0 \leq x \leq x_0$, then we obtain from the equation (2) the ratios:

$$\frac{K_z}{K_D} = \frac{F}{F_0 - \frac{S_0}{x_0}} - 1 \quad .. \quad .. \quad .. \quad (3)$$

and $$\frac{M}{K_D} = S_0 - \left(1 + \frac{K_z}{K_D}\right)\left(S_0 - \frac{J_0}{x_0}\right) \quad .. \quad (4)$$

These ratios are worked out for the solid rectangular section, the square diagonally placed section (neutral axis parallel to a diagonal) and a two-flanged section (Fig. 4) with $d = d' = \frac{3}{20}H$. In order to render the data in Fig. 5 non-dimensional and at the same time to enable a comparison to be made with the customary equation for the bending stresses, an ideal bending strength was calculated from the moment of rupture M in accordance with the formula:

$$K_B = \frac{M}{W} \quad (W = \text{moment of resistance of the cross-section of the member}) \quad (5)$$

and the ratio $K_B/K_D$ compared with $K_z/K_D$. The values $K_B/K_D = 1.57$ to $1.67$ correspond to the values $K_z/K_D = 1.8$ to $2.0$, in respect of the solid rectangular section (Fig. 5, curve $b$), in agreement with the results of Newlin and Trayer.* In respect of the square diagonally placed section (curve $a$) we get slightly higher values for the ideal bending strength, while, as regards the two-flanged section examined (curve $c$), these values are substantially lower. Thus, if it is desired to apply the formula (5) for determining the moment of rupture, either a special ideal bending strength must be attributed to each cross-section form or, better, if the bending strength has a fixed value, instead of the resistance moment W, an ideal moment of resistance $W_i = cW$ must be introduced, as was done by J. A. Newlin and G. W. Trayer.* It should be noted, however, that the "form factor" $c$ depends not only on the cross-section form but also on the ratio $K_z/K_D$.

It will also be seen from Fig. 5 that the two solid sections behave quite differently from the two-flanged section. In the latter the bending moment at fracture is scarcely influenced by any alteration in the value $K_z/K_D$ within the range, important in practice, $1.8 < K_z/K_D < 2.0$.

We shall now turn to the second type of fracture in which a dangerous compression value is reached on the pressure side, while the stress $K_z'$ of the extreme tension-fibre is still below the tensile strength $K_z$. In this type of fracture the bending moment at fracture is independent of the tensile-strength value. Thus, in Fig. 5, where both types of fracture are considered, the ideal bending strength $K_z/K_D \leq K_z'/K_D$ is indicated by the curve corresponding to the first type of fracture, but in respect of $K_z/K_D \geq K_z'/K_D$ by a horizontal straight line corresponding to the second type of fracture. A simple calculation shows that in the solid sections examined and in the practically important values of the ratio $K_z/K_D$ the neutra axis at the moment when the fracture of the first type occurs is still almost in the centre of the cross-section height. As regards these sectional forms, therefore, at the moment of the first type of fracture, the amount of the maximum compression is but little more than that of

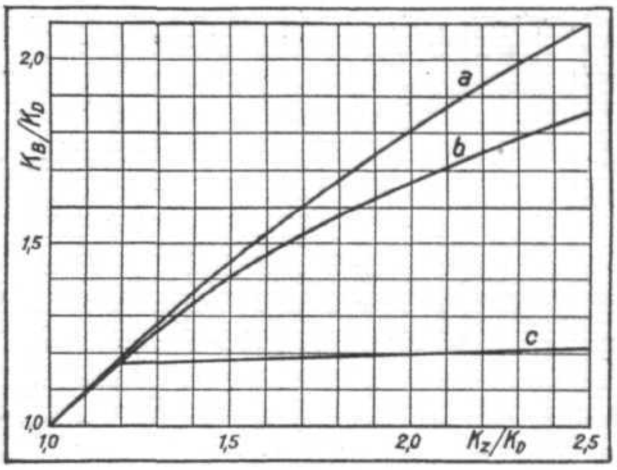


Fig. 5.

the maximum extension. As the dangerous amount of compression in any case considerably exceeds the amount of extension in the fracture test, a fracture of the second type does not therefore come into consideration in respect of the solid sections examined.

Matters are different in two-flanged sections. For equilibrium, the resultant of the pressure stresses must equal the resultant of the tensile stresses. When, therefore, tension flange and pressure flange are of the same height the mean stress in the tension flange must be equal to the stress $K_D$ present at all points of the pressure flange. In respect of $K_z/K_D = 2$, therefore, the mean stress $K_D$ in the tension flange is equal to one-half of the maximum stress $K_z$, and so the distribution of the stresses over the tension flange is represented by a triangle, while the zero line of the distribution of stresses coincides with the inner edge of the tension flange. As the ratio of the maximum compression to the maximum extension is given by the ratio of the distances of the neutral axis from the extreme pressure-fibre and the extreme tension-fibre, a fracture of the second type is therefore quite possible in the case of the two-flanged section examined. But the form of curve $c$ (Fig. 5), determined on the assumption of a fracture of the first type, diverges only very slightly from that of a horizontal straight line. Consequently, it matters little which type of fracture is considered in determining the moment of rupture.

In aircraft construction a two-flanged section with flanges of different thicknesses (Fig. 4) is frequently used as the cross-section of the spar. Making use of the results of the Newlin-Trayer experiments, A. von Baranoff† has dealt with the dimensioning of such a cross-section. We shall deal with the same problem, while applying the principles evolved here. In the dimensioning of the flanges the height H and width B of the section may be regarded as given. We therefore make the moment of rupture M non-dimensional by dividing it by the product of the resistance moment of the rectangle of height H and width B and the compressive strength $K_D$ of the wood:

$$\overline{M} = \frac{M}{\frac{BH^2}{6}K_D} \quad .. \quad .. \quad .. \quad (6)$$

Fig. 6 shows, for various ratios $d/d'$, this non-dimensional moment of rupture $\overline{M}$ in dependence on the pressure-flange

* National Advisory Committee for Aeronautics Report, No. 181 (1924).

† *A. v. Baranoff*, "Zeitschrift für Flugtechnik und Motorluftschiffahrt," No. 18 (1927), p. 81.

thickness $d/H$. The small circles on the curves in Fig. 6 indicate the limits within which a certain simple formula for the bending moment at fracture can be applied: this formula, published at an earlier date, premises that the turning point of the stress distribution lies between the inner edges of both flanges.‡ For higher $d/H$ values the equations (3) and (4) must be used for the determination of the bending moment at fracture. The three curves in Fig. 6 lie very close together. **This means that with a given height and width of section and a specified bending moment at fracture the thickness of the pressure flange depends but little on the ratio $d/d'$ of the pressure-flange thickness to the tension-flange thickness, provided, of course, that this ratio keeps within the limits customary in practice.**

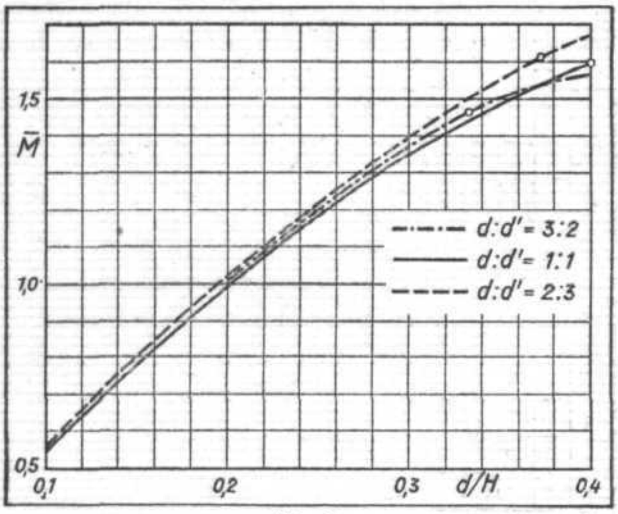


Fig. 6.

Taking as a basis the German specifications for the strength of aircraft, the two decisive values of the bending moment generally correspond to the load conditions A (pulling out from a dive) and E (pulling out from inverted flight), while the bending moment in the "A" case is much the greater. Thus, owing to the negligibility of the pressure-flange thickness in relation to the value of the ratio $d/d'$ as shown above, the top flange of the spar may be dimensioned as pressure-flange of the "A" case with the aid of Fig. 6, the three curves being replaced by a mean. The bottom flange of the spar is then dimensioned in the same manner as the compression flange of the "E" case. On the basis of the ratio $d/d'$ thus obtained the calculation could be repeated, using curves to be inserted in Fig. 6 in accordance with this ratio, but such a procedure is generally found to be unnecessary.

‡ *W. Prager*, "Zeitschrift für Flugtechnik und Motorluftschiffahrt," No. 24 (1933), p. 521.

# TECHNICAL LITERATURE

## SUMMARIES OF AERONAUTICAL RESEARCH COMMITTEE REPORTS

REPORTS published by His Majesty's Stationery Office, London, which may be purchased directly from H.M. Stationery Office at the following addresses: Adastral House, Kingsway, W.C.2; 120, George Street, Edinburgh; York Street, Manchester; 1, St. Andrew's Crescent, Cardiff; 15, Donegall Square West, Belfast; or through any ordinary bookseller.

THE FLOW DUE TO A ROTATING DISC. By W. G. Cochran. R. & M. No. 1605. (1 page.) June, 1934. Price 2d. net.

Abstract only of paper published in *Proc. Camb. Phil. Soc.*

ON THE STRESSES INDUCED BY FLEXURE IN A DEEP RECTANGULAR BEAM. By D. B. Smith and R. V. Southwell, F.R.S. R. & M. No. 1606. (1 page.) June, 1934. Price 2d. net.

Abstract of paper published in Proceedings of the Royal Society, A, Vol. 143 1934, pp. 271–284.

A MODIFICATION OF OSEEN'S APPROXIMATE EQUATION FOR THE MOTION IN TWO DIMENSIONS OF A VISCOUS INCOMPRESSIBLE FLUID. By R. V. Southwell, F.R.S., and H. D. Squire. R. & M. No. 1607. (2 pages.) June, 1934. Price 2d. net.

Abstract of paper published in the *Philosophical Trans.* of the Royal Society Series A, Vol. 232, pp. 27–64.

WINDSCREENS WITH OPENINGS. By F. B. Bradfield, M.A., and B. Lockspeiser, M.A. Communicated by the Director of Scientific Research, Air Ministry. R. & M., No. 1613. (7 pages and 7 diagrams.) December 6, 1933. Price 9d. net.

The pilot's field of view through the type of windscreen normally fitted to open cockpits deteriorates rapidly in rain or snow, or under ice-forming conditions.

Wind tunnel and full scale tests have been made on two types of windscreens with openings—the deflector windscreen and the divided windscreen. In the former a shielded area beyond the side of the screen is provided by the use of small deflectors. In the latter, the screen is divided to allow a forward rotation of the upper half accompanied by a rotation in the opposite direction of the lower half. This device enables a forward view to be obtained through a horizontal opening of adjustable width.

The deflector type windscreen provides the pilot with a shielded area about 6in. wide, enabling him to look round the side of the screen without discomfort.

The divided windscreen has been tested in flight in (*a*) fine weather, (*b*) cloud, (*c*) drizzle, (*d*) heavy rain, and (*e*) under ice-forming conditions. In all cases a good view forward was obtained.

ON THE USE OF THE HOT-WIRE TYPE OF INSTRUMENT FOR RECORDING GUSTS. By L. F. G. Simmons, M.A., A.R.C.S., and J. A. Beavan, B.A., of the Aerodynamics Department, N.P.L. R. & M., No. 1615. (16 pages and 11 diagrams.) February 1, 1934. Price 1s. net.

Experiments undertaken with the object of determining the loading imposed on machines when flying in gusty weather emphasise the need for additional information on the nature and duration of gusts. As is well known, gusts are relatively small, but intense disturbances in the atmosphere, which produce unsteadiness in the wind velocity such as are well exhibited in records of self-recording anemometers. The records, however, do not faithfully represent the velocity changes, except when these occur slowly enough to enable the instrument to follow accurately.

Continuous records of the speed and direction (vertical) of the wind at the top of a steel lattice-work tower about 64 feet high, were obtained by means of a hot-wire anemometer and a hot-wire direction meter. The records were taken on the same day and extend over a range of speeds, the highest mean speed reached being about 70 feet per second.

All the records indicate the presence of intense disturbances of short duration, which cannot be recorded by the usual methods. Like the larger disturbances these occur irregularly, without, in general, any obvious relationship existing between them. In one record, taken at a mean speed of 55 feet per second, the changes registered appear to have been caused by an eddy of about 40 feet diameter, probably due to local obstructions, passing within 10 feet of the instruments. During the time it was effective, namely, 0.8 second, the horizontal speed of the wind attained a maximum value of 125 feet per second, and the vertical component varied approximately from + 50 to − 50 feet per second.

Other records suggest the existence of eddies rotating about vertical axes, but without a yawmeter no measure of their intensity could be made.

INTERFERENCE EFFECT OF THE SURFACE OF THE SEA ON THE CHARACTERISTICS OF A FLYING BOAT. By W. L. Cowley, A.R.C.Sc., D.I.C., and G. A. McMillan, M.Eng., of the Aerodynamics Department, N.P.L. R. & M., No. 1626. (15 pages and 8 diagrams.) May 15, 1934. Price 1s. net.

Full scale flying boat experiments carried out at Felixstowe have shown that an appreciable interference effect occurs on lift when an aircraft is flying near the surface of the sea. An increase in lift would be expected from the Vortex Theory at low angles of incidence, but the theory indicates a fall in lift near the maximum. In view of the increase in lift found in the full scale experiments, a request was made for model tests to be carried out at the N.P.L.

Measurements were taken of lift, drag and pitching moment on the model of the Short R6/28 flying boat when suspended in the Duplex wind tunnel near a platform that represented the sea. The tests included experiments both with and without airscrews running. The position and attitude of the model relative to the sea were made to correspond to the taxi-ing and take-off conditions of the aircraft.

The results showed that the presence of the sea increased the maximum lift by about 6 per cent. At the lower end of the angle range the increase in lift was a greater percentage of the lift, but although the vortex theory indicates a change of lift due to a change in the angle of incidence of the aircraft, no alteration in angle was shown by the drag measurements. The increase in maximum lift also appears to be contrary to the conclusions of the vortex theory.

It is intended to study this question more extensively by means of an aerofoil alone and, in order to obtain a more direct comparison with theory, the case of infinite aspect ratio will be included.

## AN EXPLANATION.

Mr. J. F. Cuss wishes us to correct a small typing error which he failed to notice in the manuscript of his article on "Spar Design," published in the June 20, 1935, issue of *The Aircraft Engineer*. In the last paragraph of the left-hand column on page 43 occurred the words: "The $Z_1$ coefficient for the appropriate F/D ratio is given in Column (15) by dividing (11) by (13)." This should have read: "The $Z_1$ coefficient for the appropriate F/D ratio is read off chart B. The new $I/I_s$ ratio is given in Column (15) by dividing (11) by (13)."